Mutation Research - Genetic Toxicology and Environmental Mutagenesis 899 (2024) 503823

Contents lists available at ScienceDirect

Mutation Research - Genetic Toxicology and Environmental Mutagenesis

journal homepage: www.elsevier.com/locate/gentox

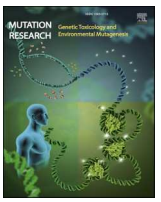

# Bleomycin-induced chromosomal aberrations in Epstein-Barr virus-transformed human lymphoblastoid cells

Andrea G. Cardozo [a], Daniel C. Castrogiovanni [b], Alejandro D. Bolzán [a,c,*]

[a] Laboratorio de Citogenética y Mutagénesis, Instituto Multidisciplinario de Biología Celular (IMBICE, CONICET-UNLP-CICPBA), calle 526 y Camino General Belgrano, La Plata, Buenos Aires B1906APO, Argentina
[b] Sector de Cultivos Celulares, Instituto Multidisciplinario de Biología Celular (IMBICE, CONICET-UNLP-CICPBA), calle 526 y Camino General Belgrano, La Plata, Buenos Aires B1906APO, Argentina
[c] Universidad Nacional de La Plata, Facultad de Ciencias Naturales y Museo, calle 60 y 122, La Plata, Buenos Aires, Argentina

ARTICLE INFO

*Keywords:*
incomplete chromosome elements
terminal acentric fragment
PNA-FISH

ABSTRACT

We have evaluated the induction of complete (i.e., without open ends) and incomplete (i.e., with non-rejoined or open ends) chromosomal aberrations by the radiomimetic antibiotic bleomycin (BLM) in human lymphoblastoid cells immortalized with the Epstein-Barr virus (EBV). An EBV-induced lymphoblastoid cell line (T-37) was exposed to BLM (10–200 μg/mL) for 2 h at 37ºC, and chromosomal aberrations were analyzed 24 h after treatment, using PNA-FISH with pan-telomeric and pan-centromeric probes. Both complete (multicentrics, rings, compound acentric fragments, and interstitial deletions) and incomplete (incomplete chromosomes or IC, and terminal acentric fragments or TAF) chromosomal aberrations increased significantly in BLM-exposed cells, although the concentration-response relationship was non-linear. Of the acentric fragments (ace) induced by BLM, 40 % were compound fragments (CF, ace +/+). TAF (ace, +/-) and interstitial fragments (IAF, ace -/-) were induced at similar frequencies (30 %). 230 ICE were induced by BLM, of which 52 % were IC and 48 % TAF. The average ratio between total incomplete chromosome elements (ICE) and multicentrics was 1.52. These findings suggest that human lymphoblastoid cells exhibit less repair capacity than human lymphocytes, with respect to BLM-induced ICE, and that chromosomal incompleteness is a common event following exposure of these cells to BLM.

## 1. Introduction

Telomere instability may result from loss of chromosome end(s) or from telomere dysfunction [1,2]. In the former case, the telomere is lost due to chromosome breaks produced at one or both ends of one or more chromosomes; this can give rise to genomic instability due to breakage-fusion-bridge cycles [1–3]. In the latter case, the telomere loses its end-capping function or becomes critically short, giving rise to a dysfunctional telomere (see [1–3] for review). True telomere loss produces non-joined or "open" chromosome ends, giving rise to incomplete chromosomes (IC, chromosomes lacking one or both ends) and terminal acentric fragments (TAF, acentric fragments derived from a chromosome break at the terminal region of a chromosome, which may be detected by FISH as fragments with telomeric signals at one end), which constitute incomplete chromosome elements (ICE) [1–3] and represent unrepaired chromosome damage. Telomere (or telomere-plus-centromere) PNA-FISH is an effective technique for detection of ICE in mammalian cells exposed to ionizing radiation or chemical mutagens [4–11].

Bleomycin (BLM, CAS No. 9041–93–4) is a radiomimetic compound with antibiotic, antitumor, and clastogenic properties, first isolated from *Streptomyces verticillus* [12]. BLM is used widely for treatment of malignancies, including testicular cancer, lymphoma, lung cancer, cervical cancer, and head-and-neck cancers [13,14]. Due to its antineoplastic properties, analysis of chromosomal instability induced by BLM is of clinical interest. Analysis of BLM-induced telomere instability is relevant

*Abbreviations:* AF/ace, acentric fragment/s; BLM, bleomycin; CAF, compound acentric fragment; EBV, Epstein-Barr virus; FISH, fluorescence *in situ* hybridization; ICE, incomplete chromosome elements; IC, incomplete chromosome; IAF, interstitial acentric fragment; PNA, peptide nucleic acid; TAF, terminal acentric fragment.

* Corresponding author at: Laboratorio de Citogenética y Mutagénesis, Instituto Multidisciplinario de Biología Celular (IMBICE, CONICET-UNLP-CICPBA, calle 526 y Camino General Belgrano, La Plata, Buenos Aires B1906APO, Argentina.
*E-mail addresses:* abolzan@imbice.gov.ar, adbolzan64@gmail.com (A.D. Bolzán).

https://doi.org/10.1016/j.mrgentox.2024.503823
Received 22 May 2024; Received in revised form 19 August 2024; Accepted 21 August 2024
Available online 25 August 2024

to understanding genomic instability induced (short- or long-term) in patients undergoing BLM-based chemotherapy. Previous work in our laboratory, using FISH with a PNA pan-telomeric probe, showed that BLM induces the formation of ICE in mammalian cells [4–6]. More recently, we found that BLM induces persistent telomere instability in rat cells, in the form of ICEs and telomere FISH signal loss/duplication, and this telomere instability persists for several generations after exposure [6]. With regard to human cells, ICE induction has only been investigated in the peripheral human lymphocytes of one individual, using PNA-FISH with pan-telomeric and pan-centromeric probes [7]. These authors found that this antibiotic induces ICE (with the ratio between ICE and multicentrics being 0.27), and an elevated proportion of interstitial acentric fragments (40 %) in relation to total acentric fragments [7]. Studies on the possible induction of telomere dysfunction-related chromosomal aberrations induced by BLM have not yet been performed in human cells.

We are carrying out experiments using a human lymphoblastoid cell line, in order to analyze the induction by BLM (short- and long-term) of complete and incomplete chromosomal aberrations, as well as telomere-dysfunction-related aberrations. Lymphoblastoid cell lines, produced by *in vitro* infection of human B-lymphocytic cells with Epstein-Barr virus, are often used in medical genetics studies, because they are a valuable tool for preserving biological material from patients possessing specific genetic aberrations. Most of these cell lines are considered EBV-transformed (rather than immortalized) cell lines, because only a few cells reach the immortalization stage (with telomerase activation, chromosomal instability, and upregulation of WRN helicase) [15–17]. EBV-transformed cells can also be used in long-term studies of mutagenesis because, unlike normal human lymphocytes, they can be continuously cultured *in vitro* for months or years [15–17].

Here, we present results concerning the short-term induction of ICE by BLM in human lymphoblastoid cells and compare our results to those previously reported in studies of normal human lymphocytes [7] and non-human cells [4–6] exposed to BLM. We applied the PNA-FISH technique with a pan-telomeric and a pan-centromeric probe to identify ICE (IC and TAF) and to distinguish between different types of acentric fragments, multicentrics (MC), and ring chromosomes, thus significantly improving the detection of all types of unstable chromosomal aberrations [1,3,18–20].

## 2. Materials and methods

### 2.1. Cell culture, drug treatments, and cell harvesting

This study was carried out using human lymphoblastoid cells (T-37 cell line, obtained from the IMBICE Cell Repository, La Plata, Buenos Aires, Argentina) [21]. This cell line was established by *in vitro* infection of human lymphocytes derived from a whole blood sample from a female donor with Epstein-Barr virus harvested from the marmoset cell line B95–8. Previous cytogenetic analysis in our laboratory showed that >90 % of T-37 cells contain 46 chromosomes [21].

Cells were grown in RPMI 1640 medium (Sigma Chemical Co., St. Louis, MO) supplemented with 20 % fetal calf serum, penicillin (100 U/mL), and streptomycin (100 μg/mL) at 37ºC in 5 % $CO_2$ atmosphere. Cells were seeded in culture medium in TC25 Corning flasks at $6 \times 10^5$ cells/mL. During the log phase of growth, cells were treated with a 2 h pulse of BLM (CAS 9041–93–4, Blocamicina®, Laboratorios Gador, Argentina, dissolved in sterile 0.9 % NaCl), 10, 25, 50, 100 or 200 μg/mL, at 37°C in order to measure concentration-dependent effects. We chose BLM concentrations similar to those used by Benkhaled et al. [7] with normal human lymphocytes. Control cultures were not exposed to BLM. Exposure time and BLM concentrations were chosen based on a previous study with T-37 cells in our laboratory [21]. At the end of the pulse treatment with BLM, the cells were washed twice with Hank's balanced salt solution and kept in culture with fresh culture medium until harvesting. To estimate cell viability, we applied the Trypan Blue exclusion assay. An aliquot of cell culture (about 30 μL) stained with 0.4 % trypan blue was used for counting viable cells in a Neubauer chamber. The remaining cells were used for cytogenetic analysis, which was performed at 24 h (first mitosis) after BLM treatment. To analyze chromosomal aberrations, colchicine (0.1 μg/mL; CAS 64–86–8; Sigma) was added to cell cultures during the last 3 h of culture. Chromosome preparations were made following standard procedures. After harvesting, cells were hypotonically shocked, fixed in methanol:acetic acid (3:1), spread onto glass slides, and processed for PNA-FISH.

### 2.2. Fluorescence in situ hybridization with PNA pan-telomeric and pan-centromeric probes (PNA-FISH)

A Cy3-conjugated PNA pan-telomeric probe [Cy3-$(CCCTAA)_3$] and a FAM-conjugated pancentromeric probe were obtained from PNA Bio (California, USA). FISH was performed according to the protocol provided by the supplier. Briefly, after pre-treatment for 10 min with 3.7 % formaldehyde and 2 mg/mL proteinase K, sample DNA was denatured at 85ºC for 10 min under a coverslip in the presence of the pan-telomeric and the pan-centromeric probe. Hybridization in a moist chamber (1 h at room temperature) was followed by two washes in 2× SSC 0.1 % Tween 20 for 10 min at 55–60°C. Afterwards, slides were mounted on an antifade reagent containing DAPI (4,6-diamidino-2-phenyl-indole) as counterstain. Fluorescence microscopy was performed on a Nikon Eclipse 50i epifluorescence microscope equipped with an HBO 100 mercury lamp, a Nikon high-resolution digital color camera (DS-Ri-U3), and filters for DAPI, FAM and Cy3 (Chroma Technology Corp, Rockingham, VT).

### 2.3. Scoring of aberrations

Chromosome analysis was performed on coded slides, and only metaphases with 46 centromeric signals were scored. Centromeres were identified using the FAM filter, whereas telomeric signals were observed using the Cy3 filter. To obtain the final three-color FISH images, DAPI, FAM, and Cy3 images were merged using ImageJ Software (version 1.52r). Since the position and number of centromeres could be easily determined with the pan-centromeric probe, all types of complete and incomplete chromosomal aberrations were scored, namely: (1) dicentric chromosomes; (2) multicentrics (those chromosomes possessing three or more centromeres; for quantification, the number of centromeres present in the polycentric chromosomes minus one was used and scored as dicentric equivalents); (3) centric rings; (4) interstitial acentric fragments (IAF, ace -/-) (i.e., chromosome elements without telomeric signals); (5) ICE, both centric (IC, +/- or -/-; IC -/- were counted as two IC +/- [7]) or acentric (TAF, ace +/-, lacking telomeric signals at one end); and (6) compound acentric fragments (CAF, ace +/+), acentric fragments labeled at both ends, i.e., exhibiting four telomeric signals [1–3]. Previous evidence [22] strongly suggests that the majority of IAFs lose the possibility of forming exchanges by the formation of a ring structure (acentric rings). Therefore, for scoring purposes, IAFs were considered complete aberrations. Chromosome breaks, gaps and chromatid exchanges (including quadriradial and triradial configurations) were excluded from the analysis. The mitotic index (MI; expressed as the percentage of cells in mitosis) was determined by analyzing 1000 cells per sample. For chromosomal aberrations analysis, cell viability and mitotic index determination, two, five, and four independent experiments (each one including one culture per sample) were performed, respectively. A total of 108–193 metaphases were analyzed for each treatment (see Tables 1–4). In the first experiment, 100 metaphases were analyzed per treatment (except in the case of BLM 200 μg/mL, where only 64 metaphases could be analyzed). In the second experiment, 79 (untreated control), 80 (BLM 10 and 25 μg/mL), 88 (BLM 50 μg/mL), 93 (BLM 100 μg/mL), and 44 (BLM 200 μg/mL) metaphases were analyzed.

**Table 1**
Number of the different pairs of incomplete chromosome elements (ICE) observed in T-37 cells following BLM treatment (μg/mL). The percentage of each type of pair is indicated between parentheses.

| Treatment | N | Pairs of ICE | | | Total |
|---|---|---|---|---|---|
| | | IC + TAF | IC + IC | TAF + TAF | |
| Control | 179 | 1 (100) | 0 | 0 | 1 |
| BLM 10 | 180 | 17 (100) | 0 | 0 | 17 |
| BLM 25 | 180 | 11 (61.1) | 2 (11.1) | 5 (27.8) | 18 |
| BLM 50 | 188 | 18*(66.7) | 6 (22.2) | 3 (11.1) | 27 |
| BLM 100 | 193 | 31 (88.6) | 2* (5.7) | 2 (5.7) | 35 |
| BLM 200 | 108 | 13 (86.7) | 2** (13.3) | 0 | 15 |

* One IC -/- was also observed.
** Two IC -/- were also observed. N, total number of metaphases analyzed; BLM, bleomycin; IC, incomplete chromosome; TAF, terminal acentric fragment. Data represent pooled values from two independent experiments.

**Table 2**
Ratio between total incomplete chromosome elements (ICE) and multicentrics (MC) observed in T-37 cells following BLM treatment (μg/mL).

| Treatment | N | Ratio ICE/MC |
|---|---|---|
| Control | 179 | 0.00 ± 0.00 |
| BLM 10 | 180 | 3.58 ± 0.91 |
| BLM 25 | 180 | 1.26 ± 0.26 |
| BLM 50 | 188 | 1.84 ± 0.72 |
| BLM 100 | 193 | 1.25 ± 0.08 |
| BLM 200 | 108 | 2.14 ± 0.14 |

N, total number of metaphases analyzed; BLM, bleomycin. For each treatment, the ratio ICE/MC corresponds to the average value (mean ± S.E.) obtained from two independent experiments.

**Table 3**
Number of the different types of acentric fragments observed in T-37 cells following BLM treatment (μg/mL). The percentage of each type of fragment is indicated between parentheses.

| Treatment | N | TAF | CAF | IAF | Total |
|---|---|---|---|---|---|
| Control | 179 | 1 (25.0) | 0 (0.0) | 3 (75.0) | 4 |
| BLM 10 | 180 | 17 (43.6) | 10 (25.6) | 12 (30.8) | 39 |
| BLM 25 | 180 | 21 (33.3) | 24 (38.1) | 18 (28.6) | 63 |
| BLM 50 | 188 | 24 (24.0) | 52 (52.0) | 24 (24.0) | 100 |
| BLM 100 | 193 | 35 (25.7) | 63 (46.3) | 38 (28.0) | 136 |
| BLM 200 | 108 | 13 (23.2) | 22 (39.3) | 21 (37.5) | 56 |

N, total number of metaphases analyzed; BLM, bleomycin; TAF, terminal acentric fragment; CAF, compound acentric fragment; IAF, interstitial acentric fragment.
Data represent pooled values from two independent experiments.

**Table 4**
Number of the different types of in excess acentric fragments observed in T-37 cells following BLM treatment (μg/mL). The percentage of each type of fragment is indicated between parentheses.

| Treatment | N | TAF | CAF | IAF | Total |
|---|---|---|---|---|---|
| Control | 179 | 1 (25.0) | 0 (0.0) | 3 (75.0) | 4 |
| BLM 10 | 180 | 17 (58.6) | 0 (0.0) | 12 (41.4) | 29 |
| BLM 25 | 180 | 11 (35.5) | 2 (6.4) | 18 (58.1) | 31 |
| BLM 50 | 188 | 20 (39.2) | 7 (13.7) | 24 (47.1) | 51 |
| BLM 100 | 193 | 31 (43.0) | 3 (4.2) | 38 (52.8) | 72 |
| BLM 200 | 108 | 13 (34.2) | 4 (10.5) | 21 (55.3) | 38 |

N, total number of metaphases analyzed; BLM, bleomycin; TAF, terminal acentric fragment; CAF, compound acentric fragment; IAF, interstitial acentric fragment.
Data represent pooled values from two independent experiments.

### 2.4. Statistical analysis of data

Statistical analysis was performed using GraphPad Prism version 9.00 software for Windows (GraphPad Software, San Diego, CA). Because different numbers of metaphases were analyzed in each experiment, the frequencies of aberrations per cell or metaphase were considered for statistical comparison of data. The significance of differences in aberration frequencies per cell among different treatments was obtained by comparing the Z score of Poisson distributions of observed ($O$) and expected ($E$) values with 95 % confidence intervals [23]. The Z score was calculated applying the following formula: $Z = O\text{-}E/\sqrt{E}$, where $O$ is the total number of chromosomal aberrations observed in the corresponding treatment, and $E = P$ x $N$ ($P$ = frequency of chromosomal aberrations per cell or metaphase observed in the untreated culture; $N$ = total number of metaphases analyzed in each sample or treatment). If the Z score is >1.96, $p<0.05$, while if Z is >2.58, $p<0.01$. One-way ANOVA with Tukey's multiple comparison test was used for comparisons between control and treated cultures (cell viability and mitotic index). In both cases, the level of statistical significance was set at $p<0.05$.

## 3. Results

### 3.1. Distribution pattern of telomeric sequences in untreated cells

This is the first use of a pan-telomeric PNA probe in T-37 cells. Therefore, before scoring aberrations, we analyzed the distribution pattern of telomeric sequences in metaphase cells from untreated cultures, after applying telomere plus centromere PNA-FISH. This analysis showed centromeric signals in all centromeres of the metaphase cells analyzed. All telomeric signals were of terminal position (no interstitial telomeric signals were observed). However, a few chromosomes exhibited telomere signal loss (telomere shortening) or duplication (telomere fragility; Fig. 1A). Thus, some telomeres in this cell line are very short for detection by PNA-FISH. More precisely, 7.4 % (13.6 per metaphase, on average) of the total number of telomeric signals expected for the 179 metaphases analyzed (considering a total of 184 telomeric signals per metaphase, typical of a normal human lymphocyte metaphase, i.e., the cell type from which lymphoblastoid cells are derived) were absent. To rule out the possibility that the lack of

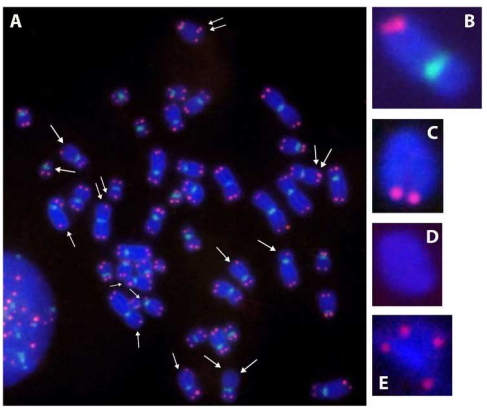


**Fig. 1.** (A) Patterns of hybridization of the pan-telomeric and pan-centromeric probes in a metaphase spread from untreated T-37 cells after PNA-FISH. Single arrows indicate sites of telomere signal loss, whereas double arrows indicate sites of telomere signal duplication. (B-D) representative examples of an incomplete chromosome and different types of acentric fragments observed in BLM-exposed cells: (B) incomplete chromosome (IC, lacking one end); (C) terminal acentric fragment (TAF, with telomeric signals at one end); (D) interstitial acentric fragment (IAF, without telomeric signals); (E) compound acentric fragment (CAF, with telomeric signals at both ends, because it results from the fusion of two TAF).

telomeric signals in the metaphase cells is due to a technical failure of the PNA-FISH technique, we performed the same procedure in slides from metaphase spreads of human lymphocytes; we found (data not shown) that all of the chromosomes exhibited their corresponding telomeric signals. Most of the telomeric signal losses (80 %) in untreated T-37 cells were of chromatid-type (i.e., a single signal loss per each chromosome end affected). Therefore, most of the chromosomes of the T-37 cell line exhibited their four telomeric signals (Fig. 1A). The frequency of telomere signal duplications in untreated T-37 cells was very low (0.28 per cell, on average).

Cytogenetic analysis of untreated T-37 cells showed that 95 % of the metaphases contained 2n=46 chromosomes, as expected from previous experiments with this cell line [21].

### 3.2. Cell viability and mitotic index

Analysis of the number of live cells (Fig. 2) and the mitotic index (Fig. 3) in each culture shows that BLM decreases cell viability and mitotic index in T-37 cells, 24 h after treatment, although these effects were not linear. Accordingly, non-significant differences were found in these parameters between 50, 100, and 200 μg/mL of BLM treatments (Fig. 2 and 3).

### 3.3. Chromosome damage

The level of chromosome damage observed in untreated T-37 cells was very low. We found only three IAF, one IC, and one TAF among 179 metaphases. This suggests that this cell line corresponds to EBV-transformed cells in a "pre-crisis" state, because the crisis stage is characterized by the presence of dicentrics and abnormal karyotypes [15,24]. As expected from previous reports with mammalian cells [4–7], BLM induced a significant concentration-dependent increase in the frequency of complete (Fig. 4) and incomplete (Fig. 5) chromosomal aberrations per metaphase compared with control cultures ($p<0.01$; Z score >2.58 for all BLM treatments compared to untreated cultures, in both experiments), although these clastogenic effects were non-linear.

The average frequency of aberrations decreased above 200 μg/mL BLM compared to 100 μg/mL BLM (Fig. 4 and 5), but non-significant

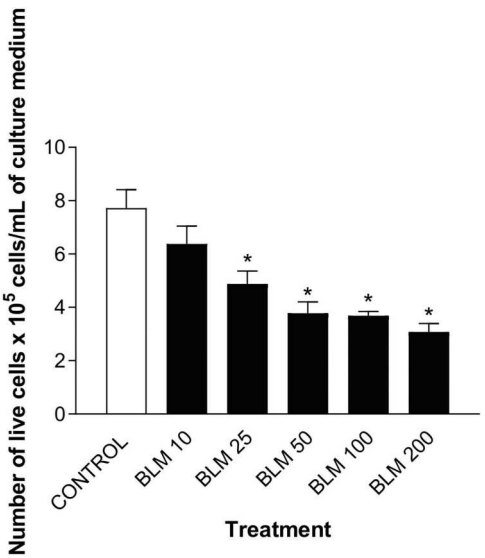


**Fig. 2.** Variation in the number of live cells observed in T-37 cells after treatment with increasing concentrations of BLM (μg/mL), as seen by the Trypan Blue assay. Data represent pooled values from five independent experiments. For each treatment, mean ± S.E. is indicated. (*) $p<0.05$ vs. untreated control culture. Statistical test: One-Way ANOVA with Tukey's multiple comparison.

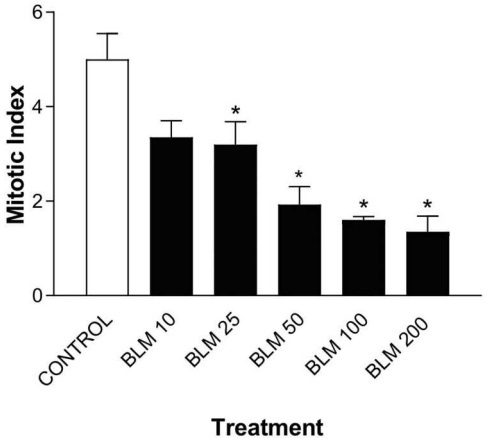


**Fig. 3.** Variation in the mitotic index observed in T-37 cells after treatment with increasing concentrations of BLM (μg/mL). Data represent pooled values from four independent experiments. For each treatment, mean ± S.E. is indicated. (*) $p<0.05$ vs. untreated control culture. Statistical test: One-Way ANOVA with Tukey's multiple comparison.

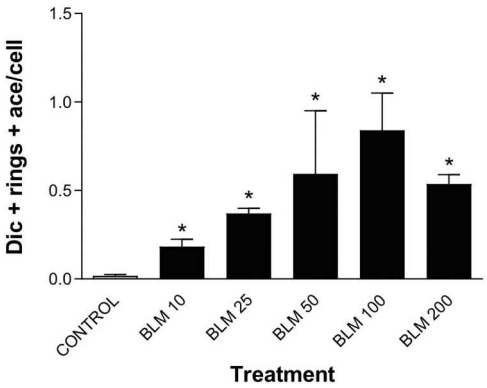


**Fig. 4.** Changes in the frequency of complete chromosomal aberrations (dicentrics, centric rings, compound fragments and interstitial fragments) per cell in T-37 cells after treatment with increasing concentrations of BLM (μg/mL). Data represent pooled values from two independent experiments. For each treatment, mean ± S.E. is indicated. The Z score of Poisson distribution indicated significant increase (*) in the frequency of aberrations induced by BLM compared with untreated (control) cultures ($p<0.01$).

differences were found between these treatments (Z score <1.96, $p>0.05$). As previously mentioned, almost 200 metaphase cells per treatment were analyzed, except for the treatment with 200 μg/mL BLM (108 metaphases), due to the elevated number of highly damaged cells found in these cultures. Moreover, the intercellular distribution of dicentrics was overdispersed, exhibiting a Poisson distribution, as previously reported for BLM in human lymphocytes [7,25] (data not shown).

The main forms of ICE observed in BLM-exposed T-37 cells were those pairs consisting of an IC (+/-) and a TAF (ace +/-), which constituted 60–100 % of the induced ICE pairs, depending on the concentration of BLM (Table 1 and Fig. 1B and 1C). Of the total number of pairs of ICE induced by BLM, 80 % were IC + TAF, 11 % IC + IC (plus a CF) and 9 % TAF + TAF (plus a dicentric or centric ring) (Table 1). Considering those IC (-/-) as two IC (+/-), the total number of ICE induced by BLM was 230 (52 % IC and 48 % TAF). The ratio between total ICE and multicentrics was on average 1.52 (range = 1.25–3.58), being much higher in BLM 10 μg/mL than at the other BLM concentrations (Table 2). This finding indicates that, for all concentrations of BLM, the frequency of induced ICE was higher than the frequency of multicentrics. The increase in both the percentage of the different forms of ICE and the ratio ICE/multicentrics was concentration dependent but

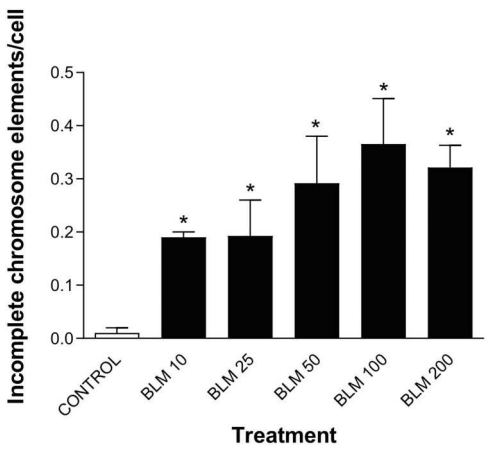


**Fig. 5.** Changes in the frequency of incomplete chromosome elements (ICE = IC and TAF) per cell in T-37 cells after treatment with increasing concentrations of BLM (μg/mL). Data represent pooled values from two independent experiments. For each treatment, mean ± S.E. is indicated. The Z score of Poisson distribution indicated significant increase (*) in the frequency of chromosomal aberrations induced by BLM compared with untreated (control) cultures ($p<0.01$).

non-linear (Tables 1 and 2).

We observed 394 acentric fragments in BLM-exposed T-37 cells; TAF (ace +/-) (Fig. 1C) and IAF (ace -/-) (Fig. 1D) were induced by BLM at similar frequencies, each representing on average 30 % of the total acentric fragments induced, whereas CAF (ace +/+) (Fig. 1E) were induced at a higher frequency, representing on average 40 % of the total number of acentric fragments induced (Table 3). However, when only "in excess" acentric fragments (i.e., those acentric fragments not accompanying the formation of dicentrics or rings) were considered, clearly IAF (51 % on average) were the most frequent type of acentric fragment induced by BLM (Table 4). The percentages of the different types of acentric fragments induced by BLM were concentration dependent but non-linear (Tables 3 and 4).

## 4. Discussion

Our findings agree with previous reports indicating the presence of telomere aberrations (mainly telomere signal loss and duplications) in EBV-induced human lymphoblastoid cell lines [17,24,26,27], due to telomere dysfunction. Although telomere signal loss could affect the scoring of the type of aberrations analyzed in the present work (and in similar works using EBV-induced lymphoblastoid cells or other cells lines with telomere dysfunction), this could only affect the scoring of acentric fragments, because the scoring of dicentrics, multicentrics and centric rings depends mainly on the presence of centromeric signals. However, even in the case of TAFs or CAFs lacking one or more telomeric signals, the presence of the accompanying aberration (IC, dicentric, multicentric, centric ring) allows one to elucidate the type of acentric fragment that was induced (a true IAF cannot be the result of an IC, a dicentric, or a centric ring). (The critical scenario could be an apparent IAF confounded with a true TAF lacking its two telomeric signals or a true CAF lacking its four telomeric signals).

Most of the expected telomeric signals (92.6 %) were present in the T-37 cell line. Therefore, the lack of some telomeric signals in the T-37 cell line did not prevent us from analyzing chromosomal aberrations.

By using telomere-plus-centromere PNA-FISH, we found that BLM induces both complete and incomplete chromosomal aberrations in EBV-transformed human lymphoblastoid cells, which exhibit telomere dysfunction. Our findings agree with the results of Benkhaled et al. [7] in normal human lymphocytes exposed to BLM, indicating that this compound induces ICE, and that the intercellular distribution of dicentrics is overdispersed. However, the increase in the frequency of both, complete and incomplete chromosomal aberrations induced by BLM in T-37 cells was not linear, whereas in the case of human lymphocytes [7] and Chinese hamster embryo (CHE) cells [4] exposed to this antibiotic, this effect was linear.

Clearly, a saturation phenomenon occurred in T-37 cells after exposure BLM concentrations > 50 μg/mL. The non-linear response in the frequency of chromosomal aberrations (and also in cell viability and mitotic index) induced by BLM in T-37 cells could be due to the presence of different subpopulations of cells with differential sensitivity to this compound (due to differential cell repair ability) [14,28] and/or differential ability of BLM uptake [14,29] in this cell line.

Our results differ in several aspects from data previously reported for human lymphocytes [7] and non-human cells [4–6]. A comparison of these data is presented in Table 5. Unfortunately, a precise comparison cannot be made, because different treatment conditions were used for studying the clastogenic effects of BLM in human cells and non-human cells (Table 5). Previous studies demonstrated that, under similar experimental conditions, human cells are more resistant than other mammalian cells to the clastogenic effects of BLM [14].

Comparing data for various mammalian cell types exposed to BLM allows several conclusions to be drawn. First, the ratio between total ICE and multicentrics in T-37 cells exposed to BLM is on average 1.52, much higher than reported by Benkhaled et al. [7] for human lymphocytes (0.27; similar to the ratio ICE/multicentrics reported for human lymphocytes exposed to low-LET ionizing radiations, 0.38 [8,9]). Since ICE represent the unrepaired chromosome damage, our results suggest that the initial damage by BLM in EBV-induced lymphoblastoid cells can be better compared to that induced by high-LET ionizing radiation (ratio ICE/multicentrics = 1.00) [10], rather than low-LET radiation (as is the case for BLM in normal human lymphocytes). Our finding regarding the ICE/multicentrics ratio indicates that EBV-transformed cells are much more sensitive to BLM than are normal human lymphocytes, in terms of ICE induction (i.e., BLM produces more unrepaired damage in EBV-transformed cells) and suggests that human lymphoblastoid cells exhibit less repair capacity than human lymphocytes regarding ICE. The greater sensitivity of EBV-transformed cells to BLM could be due to the oxidative stress previously induced by the virus, as reported elsewhere [26,30–32], although further experiments are needed to test this possibility. Despite the above findings, a ratio of ICE/multicentrics of 27.6 has been reported for BLM-treated CHE cells [5], indicating that Chinese hamster cells are much more sensitive to this compound in terms of ICE than both human lymphocytes and human lymphoblastoid cells. The different sensitivity to BLM of CHE cells compared to human cells could be attributed to various factors - particularly different cell repair ability- as suggested by Benkhaled et al. [7]. ICE induction by BLM has also been observed in rat adipocytes [6] and domestic rabbit embryo cells [5], but this compound did not induce multicentrics in these cells, preventing us from establishing an ICE/multicentrics ratio.

Second, the relative proportion of the two forms of ICE, i.e., IC and TAF, induced by BLM in T-37 cells was 52 % IC and 48 % TAF, very similar to those previously reported for human lymphocytes [7] and other mammalian cells [4–6] exposed to this antibiotic (Table 5). This indicates that BLM induces IC and TAF in a similar proportion, no matter the cell type exposed to this compound, with a slight predominance of IC over TAF.

Third, BLM induces a different proportion of the different types of pairs of ICE, depending on the cell type exposed (Table 5). Whereas Benkhaled et al. [7] reported 46 % IC + TAF, 31 % IC + IC, and 23 % TAF + TAF for human lymphocytes, in T-37 cells we observed that pairs of IC + TAF were almost 10 × more frequent than TAF + TAF pairs (Table 5). Pairs of IC + TAF also predominate in rat (85 %) [6], domestic rabbit (99 %) [5] and Chinese hamster cells (98–99 %) [4,5] exposed to BLM (Table 5), as well as in human lymphocytes exposed to low-LET (68 %) [8] and high-LET radiations (45 %) [10]. If we assume that pairs of IC (+/-) or TAF (+/-) originated from an incomplete exchange, whereas

**Table 5**
Relative comparison between human cells and other mammalian cells regarding their chromosomal sensitivity to BLM in terms of incomplete (represented by IC and TAF) and complete (represented by MC) chromosomal aberrations, as evaluated by telomere (T-FISH) or telomere plus centromere (T+C-FISH) PNA-FISH.

| Cell type | Experimental conditions | N | Ratio ICE/MC | % of each type of ICE | % of each type of pairs of ICE | % of each type of AF |
|---|---|---|---|---|---|---|
| Human lymphoblastoid cells (this work)* | T+C-FISH | 849 | 1.52 | 52 % IC | 80 % IC+TAF | 40 % CAF |
| | BLM (10–200 μg/mL) | | | 48 % TAF | 11 % IC+IC | 30 % TAF |
| | 2 h treatment | | | | 9 % TAF+TAF | 30 % IAF |
| Human lymphocytes [7]* | T+C-FISH | 451 | 0.27 | 54 % IC | 46 % IC+TAF | 55 % CAF |
| | BLM (30–120 μg/mL) | | | 46 % TAF | 31 % IC+IC | 5 % TAF |
| | 3 h treatment | | | | 23 % TAF+TAF | 40 % IAF |
| Rat adipocytes [6] | T-FISH | 133 | 0.00** | 57 % IC | 85 % IC+TAF | 4 % CAF |
| | BLM (2.5 μg/mL) | | | 43 % TAF | 15 % IC+IC | 86 % TAF |
| | 30 min treatment | | | | | 10 % IAF |
| Chinese hamster embryo cells [5] | T-FISH | 201 | 27.6 | 50 % IC | 98 % IC+TAF | 0.7 % CAF |
| | BLM (2.5 μg/mL) | | | 50 % TAF | 1.5 % IC+IC | 74 % TAF |
| | 30 min treatment | | | | 0.5 % TAF+TAF | 25.3 % IAF |
| Domestic rabbit embryo cells [5] | T-FISH | 273 | 0.00** | 51 % IC | 99 % IC+TAF | 1 % CAF |
| | BLM (2.5 μg/mL) | | | 49 % TAF | 1 % IC+IC | 89 % TAF |
| | 30 min treatment | | | | | 10 % IAF |
| Chinese hamster embryo cells [4]* | T-FISH | 1389 | ND | 51 % IC | 99 % IC+TAF | 12 % CAF |
| | BLM (1–7.5 μg/mL) | | | 49 % TAF | 1 % IC+IC | 41 % TAF |
| | 30 min treatment | | | | | 47 % IAF |

* In these cases, all the parameters showed in the Table were considered taking into account the total number of chromosomal aberrations (IC+TF vs. MC) induced by all the concentrations of BLM used in the study.

** No multicentrics were induced in these cells. N, total number of metaphases analyzed; BLM, bleomycin; ICE, incomplete chromosome elements (i.e., IC+TAF); MC, multicentrics; AF, acentric fragment; IC, incomplete chromosome; TAF, terminal acentric fragment; CAF, compound acentric fragment; IAF, interstitial acentric fragment. ND, not precisely determined (however, as reported in ref. [4], the frequency of ICE was always higher than the frequency of multicentrics). In all cases, BLM treatments were made at 37ºC, and cells were harvested in their first mitosis after treatment (i.e., short-term effect).

pairs of IC + TAF originated from a terminal deletion [7,8], we can conclude that terminal deletions predominate in EBV-transformed human cells as well as non-human cells exposed to BLM, whereas in normal human lymphocytes exposed to this compound incomplete exchanges and terminal deletions contribute equally to ICE.

Finally, we found that BLM induced more CAF (40 %) than IAF and TAF (30 % each) in human lymphoblastoid cells. On the contrary, a higher percentage of CAF (55 %) and IAF (40 %), and a small proportion of TAF (5 %) was reported for human lymphocytes exposed to BLM [7]. However, our present results support those of Benkhaled et al. [7], indicating that the elevated proportion of IAF in relation to total acentric fragments induced by BLM could be a characteristic signature of the clastogenic effect of this compound (γ-rays induced 14 % [9], X-rays 26 % [8], and α-particles 17 % [10] of IAF). Accordingly, we found that IAF constitutes 51 % of all the "in excess" acentric fragments induced by BLM in T-37 cells (Table 4). In contrast, most studies with non-human cells exposed to BLM showed that TAF are the predominant type of AF (Table 5). Further experiments are needed to determine why mammalian cells exhibit differences in their capacity to repair BLM-induced ICE and in the proportion of the different types of BLM-induced AF.

In conclusion, our results suggest that human lymphoblastoid cells are more sensitive to BLM and exhibits less repair capacity than normal human lymphocytes, in terms of ICE. Therefore, the data obtained using normal human lymphocytes should not be extrapolated to EBV-transformed human lymphocytes. Further studies will be needed to explore in more detail the chromosomal sensitivity of mammalian cells to BLM. In particular, it will be important to determine whether BLM-induced ICE (i.e., unrepaired chromosome damage) persist in the long-term in EBV-induced lymphoblastoid cells -as previously reported in rat adipocytes [6]-, and whether this compound induces short- and long-term telomere dysfunction-related chromosomal aberrations in these cells (more precisely, if BLM enhances the telomere dysfunction already present in these cells). The study of long-term clastogenic effects of BLM in human cells may be of medical relevance, particularly for clinical chemotherapies based on this compound, due to the potential risks of tumorigenesis associated with BLM-induced telomere instability. In this context, it will be important to determine the persistence of ICE and other forms of telomere instability in the progeny of human cells exposed to BLM. Such experiments are currently in progress in our laboratory.

## CRediT authorship contribution statement

**Andrea G. Cardozo:** Writing – review & editing, Methodology, Investigation. **Daniel C. Castrogiovanni:** Writing – review & editing, Methodology, Investigation. **Alejandro Daniel Bolzán:** Writing – review & editing, Writing – original draft, Methodology, Investigation, Funding acquisition, Conceptualization.

## Declaration of Competing Interest

The authors declare that they have no known competing financial interests or personal relationships that could have appeared to influence the work reported in this paper.

## Data Availability

Data will be made available on request.

## Acknowledgments

This work was supported by grants from CONICET (PIP No. 0182), CICPBA and UNLP of Argentina. We wish to thank Federico Sedelli, Eugenio Cálcena and Julieta Parisi for technical assistance, and Alejandro Portela (Lab. Gador, Argentina) for providing us the bleomycin samples.

## References

[1] A.D. Bolzán, Using telomeric chromosomal aberrations to evaluate clastogen-induced genomic instability in mammalian cells, Chromosome Res 28 (2020) 259–276.
[2] A.D. Bolzán, Considerations on the scoring of telomere aberrations in vertebrate cells detected by telomere or telomere plus centromere PNA-FISH, Mutat. Res. 794 (2024) 108507.
[3] A.D. Bolzán, Chromosomal aberrations involving telomeres and interstitial telomeric sequences, Mutagenesis 27 (2012) 1–15.
[4] A.D. Bolzán, M.S. Bianchi, Detection of incomplete chromosome elements and interstitial fragments induced by bleomycin in hamster cells using a telomeric PNA probe, Mutat. Res. 554 (2004) 1–8.

[5] M.C. Díaz-Flaqué, M.S. Bianchi, A.D. Bolzán, A comparative analysis of bleomycin-induced incomplete chromosome elements in two mammalian cell lines using a telomeric PNA probe, Environ. Mol. Mutagen. 47 (2006) 674–681.
[6] N.S. Paviolo, I.Y. Quiroga, D.C. Castrogiovanni, M.S. Bianchi, A.D. Bolzán, Telomere instability is present in the progeny of mammalian cells exposed to bleomycin, Mutat. Res. 734 (2012) 5–11.
[7] L. Benkhaled, M. Xunclá, M.R. Caballín, L. Barrios, J.F. Barquinero, Induction of complete and incomplete chromosome aberrations by bleomycin in human lymphocytes, Mutat. Res. 637 (2008) 134–141.
[8] J.J.W.A. Boei, S. Vermeulen, A.T. Natarajan, Analysis of radiation-induced chromosomal aberrations using telomeric and centromeric PNA probes, Int. J. Radiat. Biol. 76 (2000) 163–167.
[9] L. Benkhaled, L. Barrios, M. Mestres, M.R. Caballin, M. Ribas, J.F. Barquinero, Analysis of gamma-rays induced chromosome aberrations: a fingerprint evaluation with a combination of pan-centromeric and pan-telomeric probes, Int. J. Radiat. Biol. 82 (2006) 869–875.
[10] M. Mestres, M.R. Caballin, E. Schmid, G. Stephan, R. Sachs, L. Barrios, J. F. Barquinero, Analysis of α-particle induced chromosome aberrations in human lymphocytes, using pan-centromeric and pan-telomeric probes, Int. J. Radiat. Biol. 80 (2004) 737–744.
[11] M. Pujol-Canadell, R. Puig, G. Armengol, L. Barrios, J.F. Barquinero, Chromosomal aberration dynamics through the cell cycle, DNA Repair 89 (2020) 102838.
[12] L.F. Povirk, M.J.F. Austin, Genotoxicity of bleomycin, Mutat. Res. 257 (1991) 127–143.
[13] J. Chen, J. Stubbe, Bleomycins: towards better therapeutics, Nat. Rev. Cancer 5 (2005) 102–112.
[14] A.D. Bolzán, M.S. Bianchi, DNA and chromosome damage induced by bleomycin in mammalian cells: an update, Mutat. Res. 775 (2018) 51–62.
[15] C.M. Counter, F.M. Botelho, P. Wang, C.B. Harley, S. Bacchetti, Stabilization of short telomeres and telomerase activity accompany immortalization of Epstein-Barr virus-transformed human B lymphocytes, J. Virol. 68 (1994) 3410–3414.
[16] M. Sugimoto, H. Tahara, T. Ide, Y. Furuichi, Steps involved in immortalization and tumorigenesis in human B-lymphoblastoid cell lines transformed by Epstein-Barr virus, Cancer Res 64 (2004) 3361–3364.
[17] M. Volleth, M. Zenker, I. Joksic, T. Liehr, Long-term culture of EBV-induced human lymphoblastoid cell lines reveals chromosomal instability, J. Histochem. Cytochem. 68 (2020) 239–251.
[18] R. M'Kacher, E.E. Maalouf, M. Ricoul, L. Heidingsfelder, E. Laplagne, C. Cuceu, W. M. Hempel, B. Colicchio, A. Dieterlen, L. Sabatier, New tool for biological dosimetry: Reevaluation and automation of the gold standard method following telomere and centromere staining, Mutat. Res. 770 (2014) 45–53.
[19] R. M'Kacher, B. Colicchio, S. Junker, E. El Maalouf, L. Heidingsfelder, A. Plesch, A. Dieterlen, E. Jeandidier, P. Carde, P. Voisin, High resolution and automatable cytogenetic biodosimetry using in situ telomere and centromere hybridization for the accurate detection of DNA damage: An overview, Int. J. Mol. Sci. 24 (2023) 5699.
[20] G.Y.Q. Ng, M.P. Hande, Use of peptide nuclei acid probe to determine telomere dynamics in improving chromosome analysis in genetic toxicology studies, Mutat. Res. 897 (2024) 503773.
[21] A. Mira, E.M. Giménez, A.D. Bolzán, M.S. Bianchi, D.M. López-Larraza, Effect of thiol compounds on bleomycin-induced DNA and chromosome damage in human cells, Arch. Environ. Occup. Health 68 (2013) 107–116.
[22] J.J.W.A. Boei, A.T. Natarajan, Combined use of chromosome painting and telomere detection to analyse radiation induced chromosomal aberrations in mouse splenocytes, Int. J. Radiat. Biol. 73 (1998) 125–133.
[23] R.A. Fisher, F. Yates. Statistical Tables for Biological, Agricultural and Medical Research, 5th Edition, Oliver & Boyd, London, 1957, p. 61.
[24] S. Lacoste, E. Wiechec, A.G. Dos Santos Silva, A. Guffei, G. Williams, M. Lowbeer, K. Benedek, M. Henriksson, G. Klein, S. Mai, Chromosomal rearrangements after *ex vivo* Epstein-Barr virus (EBV) infection of human B cells, Oncogene 29 (2010) 503–515.
[25] A.D. Bolzán, M.S. Bianchi, E.M. Giménez, M.C. Díaz Flaqué, V.R. Ciancio, Analysis of spontaneous and bleomycin-induced chromosome damage in peripheral lymphocytes of long-haul aircrew members from Argentina, Mutat. Res. 639 (2008) 64–79.
[26] S.A. Kamranvar, M.G. Masucci, The Epstein-Barr virus nuclear antigen-1promotes telomere dysfunction via induction of oxidative stress, Leukemia 25 (2011) 1017–1025.
[27] S.A. Kamranvar, X. Chen, M.G. Masucci, Telomere dysfunction and activation of alternative lengthening of telomeres in B-lymphocytes infected by Epstein-Barr virus, Oncogene 32 (2013) 5522–5530.
[28] K. Valerie, L.F. Povirk, Regulation and mechanisms of mammalian double-strand break repair, Oncogene 22 (2003) 5792–5812.
[29] K. Sidik, M.J. Smerdon, Bleomicyn-induced DNA damage and repair in human cells permeabilized with lysophosphatidylcoline, Cancer Res 50 (1990) 1613–1619.
[30] F. Cerimele, T. Battle, R. Lynch, D.A. Frank, E. Murad, C. Cohen, N. Macaron, J. Sixbey, K. Smith, R.S. Watnick, A. Eliopoulos, B. Shehata, J.L. Arbiser, Reactive oxygen signaling and MAPK activation distinguish Epstein–Barr Virus (EBV)-positive versus EBV-negative Burkitt's lymphoma, Proc. Natl. Acad. Sci. USA 102 (2005) 175–179.
[31] M.C. Belfiore, A. Natoni, R. Barzellotti, N. Merendino, G. Pessina, L. Ghibelli, G. Gualandi, Involvement of 5-lipoxygenase in survival of Epstein–Barr virus (EBV)-converted B lymphoma cells, Cancer Lett. 254 (2007) 236–243.
[32] B. Gruhne, R. Sompallae, D. Marescotti, S.A. Kamranvar, S. Gastaldello, M. G. Masucci, The Epstein–Barr virus nuclear antigen-1 promotes genomic instability via induction of reactive oxygen species, Proc. Natl. Acad. Sci. USA 106 (2009) 2313–2318.